# Measurement of Vector and Tensor Asymmetries in Quasielastic (e,e'p) Electron Scattering from Deuterium

- Deuteron structure theoretically calculable to high precision
- The BLAST Experiment D.K. Hasell *et al*., Ann. Rev. Nucl. Part. Sci. **61**, 409 (2011)
- Quasielastic (e,e'p) Results A. DeGrush *et al*. Phys. Rev. Lett. **119**, 182501 (2017)
- Conclusions

# The Spin Structure of the Deuteron

J=1

L=0
S=1

**1 = L + S**

L=2
S=3/2

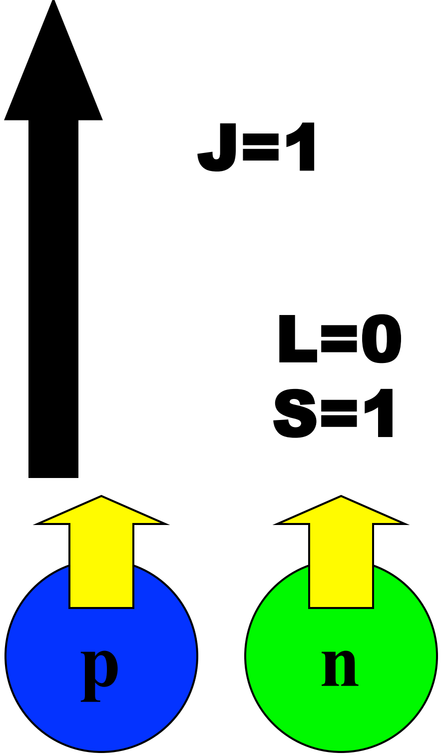


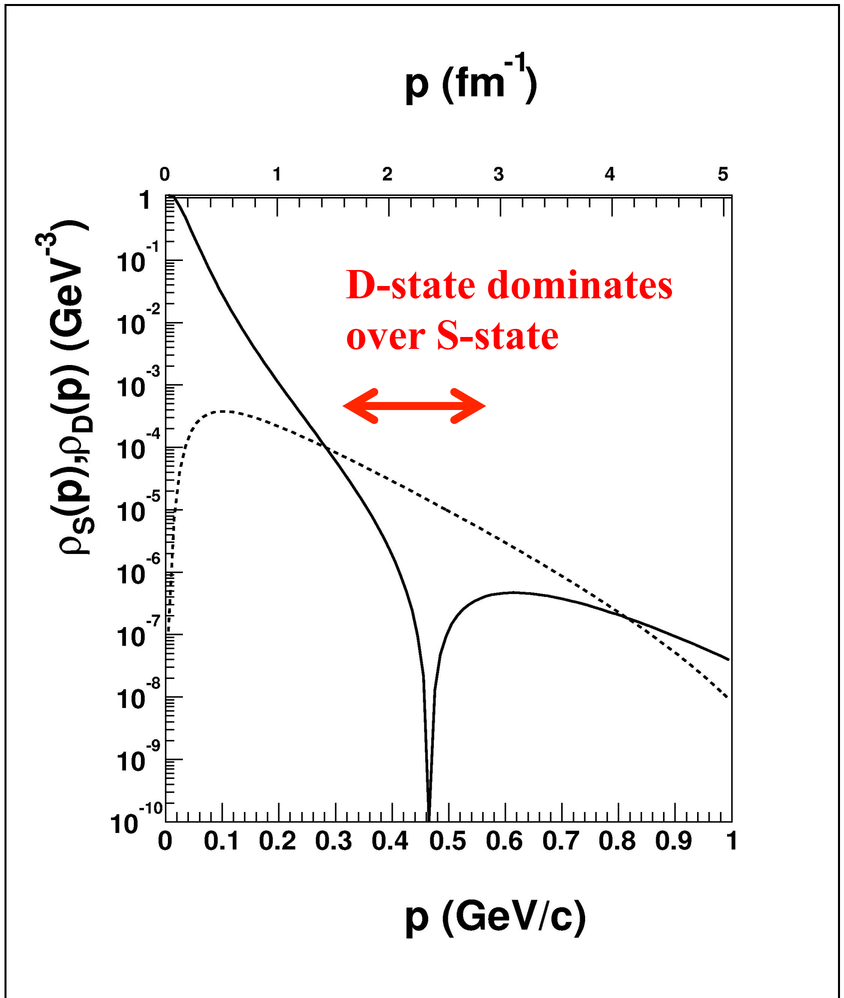


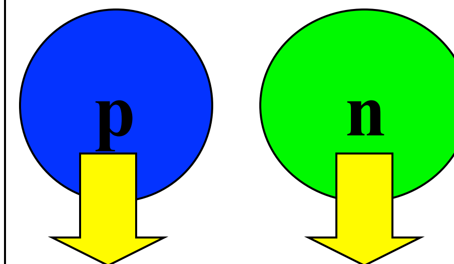


**S-state 96% of g.s. wave function**

**D-state 4% of g.s. wave function**

PHYSICAL REVIEW C VOLUME 54, NUMBER 2 AUGUST 1996

# Femtometer toroidal structures in nuclei

J.L. Forest, V.R. Pandharipande, S.C. Pieper, R.B. Wiringa, R. Schiavilla, A. Arriaga

## Nucleon-nucleon potential

$$v_{0,1} = v^{c}_{0,1}(r) + \underline{v^{t}_{0,1}(r) S_{ij}} + v^{ls}_{0,1}(r)\mathbf{L}\cdot\mathbf{S} + v^{l2}_{0,1}(r)L^2 + v^{ls2}_{0,1}(r)(\mathbf{L}\cdot\mathbf{S})^2,$$

tensor force

- θ is the polar angle of **r** wrt the spin quantization axis
- Strong effect of the tensor force on NN potential depending on different $M_s$ sub-states
- Equidensity surfaces have very different structures depending on $M_s$

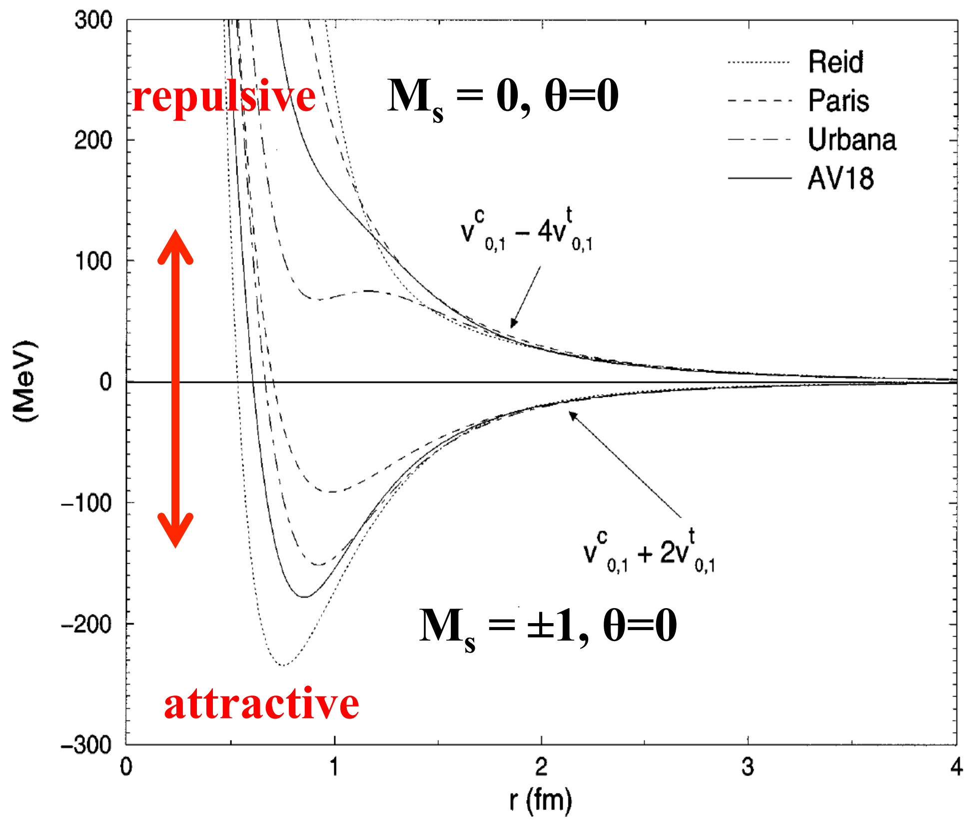

# Equidensity Surfaces having $\rho_d^{\pm 1} = 0.24\ \mathrm{fm}^{-3}$ (A) and $\rho_d^{0} = 0.24\ \mathrm{fm}^{-3}$ (B)

**In the absence of the tensor force, the equidensity surfaces are concentric spheres**

**Repulsive NN core**

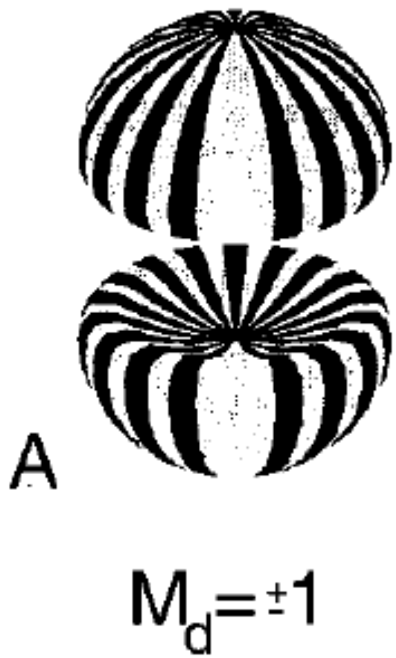


**Dumbbell**

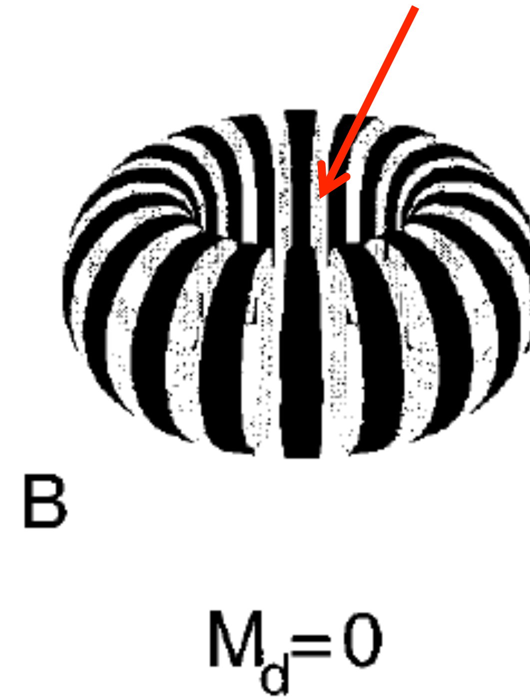


**Torus**

**Angular confinement due to tensor force**

# Predictions for Quasielastic (e,e'p)

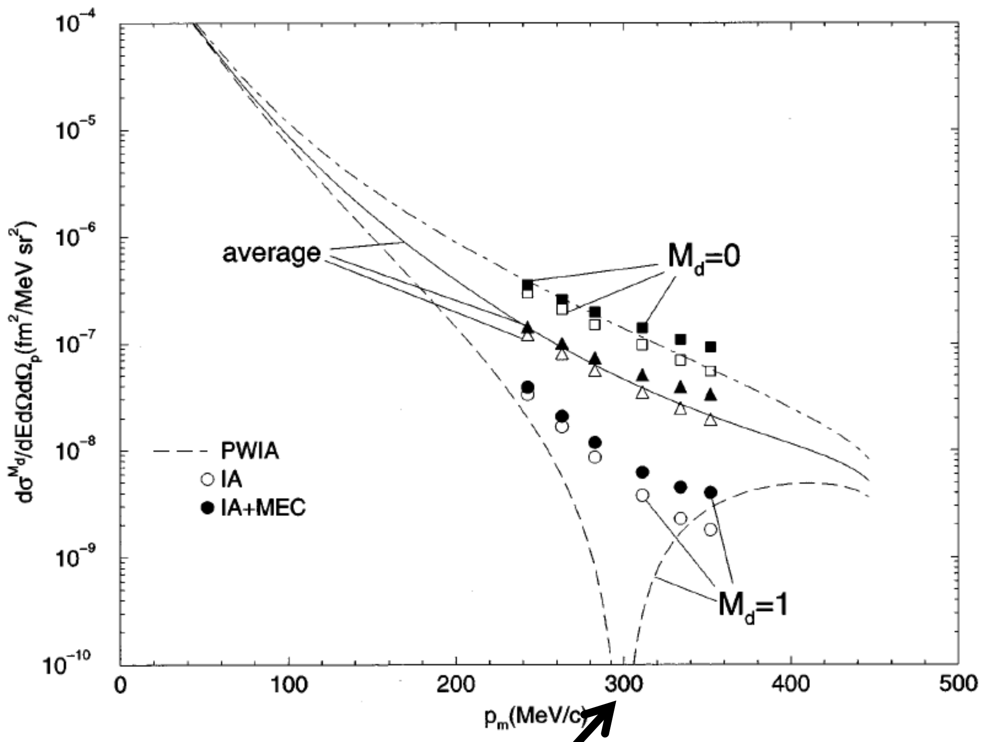


FIG. 12. The calculated values of $\vec{d}(e,e'p)n$ cross section for the kinematics described in the text. Hollow and full symbols indicate results of complete calculations without and with meson-exchange currents.

**Zero around 300 MeV/c!**

PRL 119, 182501 (2017) PHYSICAL REVIEW LETTERS week ending 3 NOVEMBER 2017

# Measurement of the Vector and Tensor Asymmetries at Large Missing Momentum in Quasielastic $(\vec{e},e'p)$ Electron Scattering from Deuterium

A. DeGrush,[1] A. Maschinot,[1] T. Akdogan,[1,‡] R. Alarcon,[2] W. Bertozzi,[1] E. Booth,[3] T. Botto,[1] J. R. Calarco,[4] B. Clasie,[1] C. Crawford,[5] K. Dow,[1] M. Farkhondeh,[1] R. Fatemi,[5] O. Filoti,[4] W. Franklin,[1] H. Gao,[6] E. Geis,[2] S. Gilad,[1] D. K. Hasell,[1,*] P. Karpius,[4] M. Kohl,[7] H. Kolster,[1] T. Lee,[4] J. Matthews,[1] K. McIlhany,[8] N. Meitanis,[1] R. Milner,[1] J. Rapaport,[9] R. Redwine,[1] J. Seely,[1] A. Shinozaki,[1] A. Sindile,[4] S. Širca,[10] E. Six,[2] T. Smith,[11] B. Tonguc,[2] C. Tschalär,[1] E. Tsentalovich,[1] W. Turchinetz,[1,†] Y. Xiao,[1] W. Xu,[6] Z.-L. Zhou,[1] V. Ziskin,[1] and T. Zwart[1]

(BLAST Collaboration)

[1]*Laboratory for Nuclear Science and Bates Linear Accelerator Center, Massachusetts Institute of Technology, Cambridge, Massachusetts 02139, USA*
[2]*Arizona State University, Tempe, Arizona 85287, USA*
[3]*Boston University, Boston, Massachusetts 02215, USA*
[4]*University of New Hampshire, Durham, New Hampshire 03824, USA*
[5]*University of Kentucky, Lexington, Kentucky 40504, USA*
[6]*Triangle Universities Nuclear Laboratory and Duke University, Durham, North Carolina 27708, USA*
[7]*Hampton University, Hampton, Virginia 23668, USA and Thomas Jefferson National Accelerator Facility, Newport News, Virginia 23606, USA*
[8]*United States Naval Academy, Annapolis, Maryland 21402, USA*
[9]*Ohio University, Athens, Ohio 45701, USA*
[10]*Faculty of Mathematics and Physics, University of Ljubljana, and Jožef Stefan Institute, 1000 Ljubljana, Slovenia*
[11]*Dartmouth College, Hanover, New Hampshire 03755, USA*

# MIT-Bates Linear Accelerator Center

**DOE Nuclear Physics**
**National User Facility**
**1974-2005**

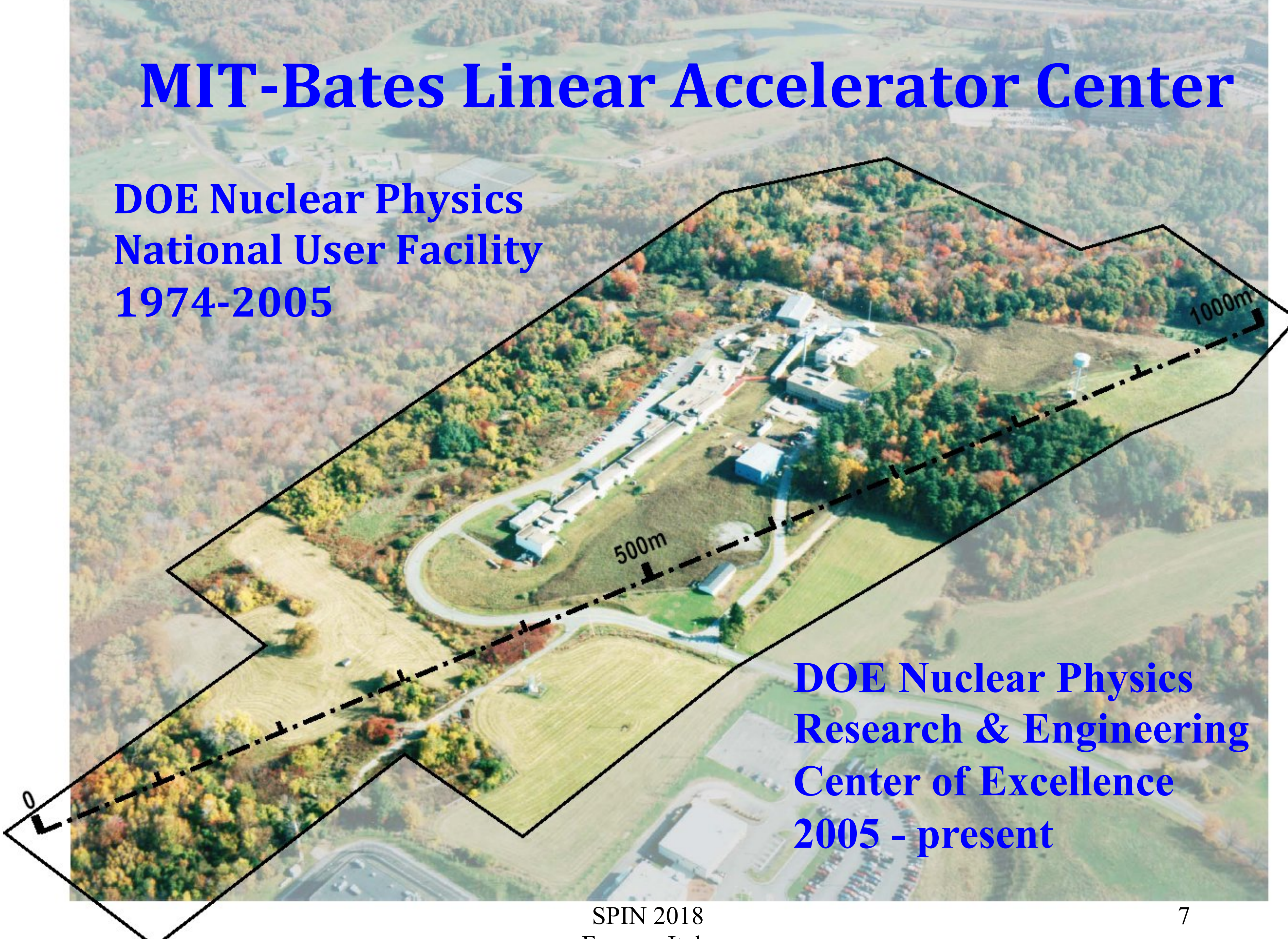


**DOE Nuclear Physics**
**Research & Engineering**
**Center of Excellence**
**2005 - present**

# MIT-Bates Linear Accelerator

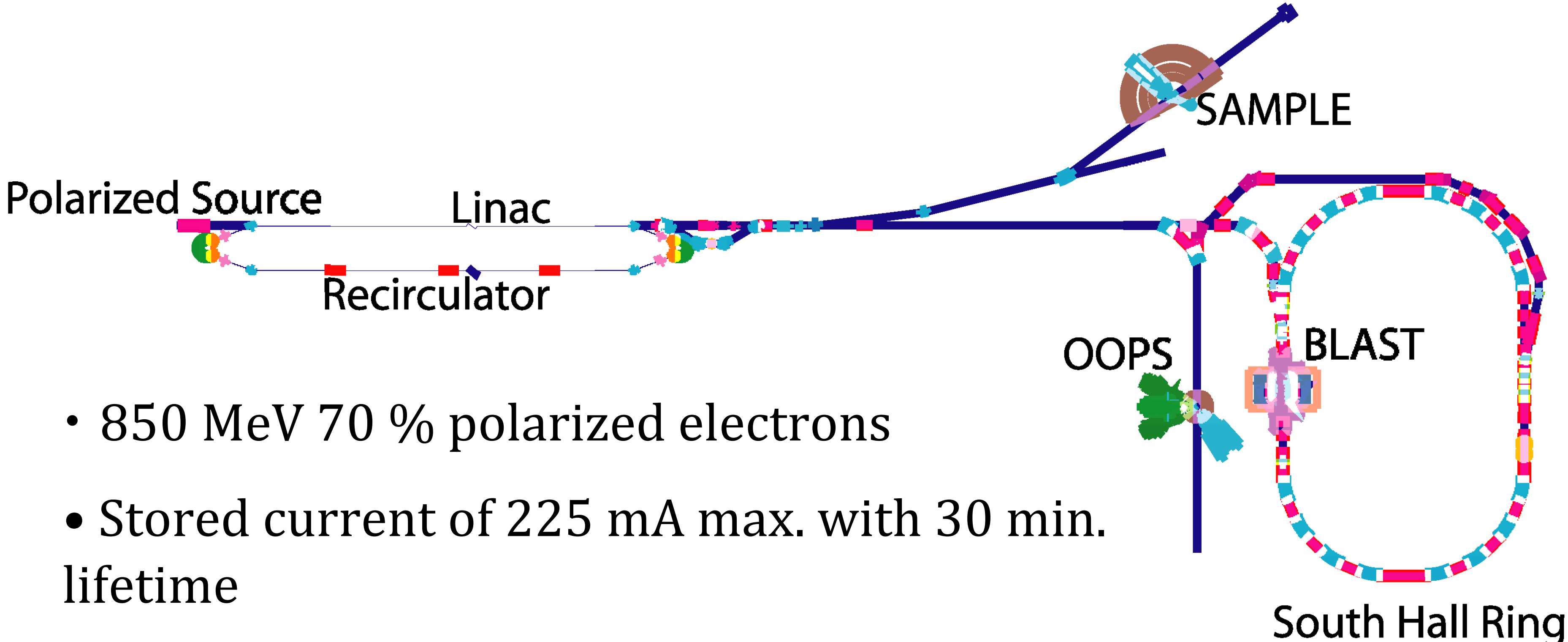


- 850 MeV 70 % polarized electrons
- Stored current of 225 mA max. with 30 min. lifetime
- Siberian snake
- Spin flipper
- Compton polarimeter

# Internal Target Concept

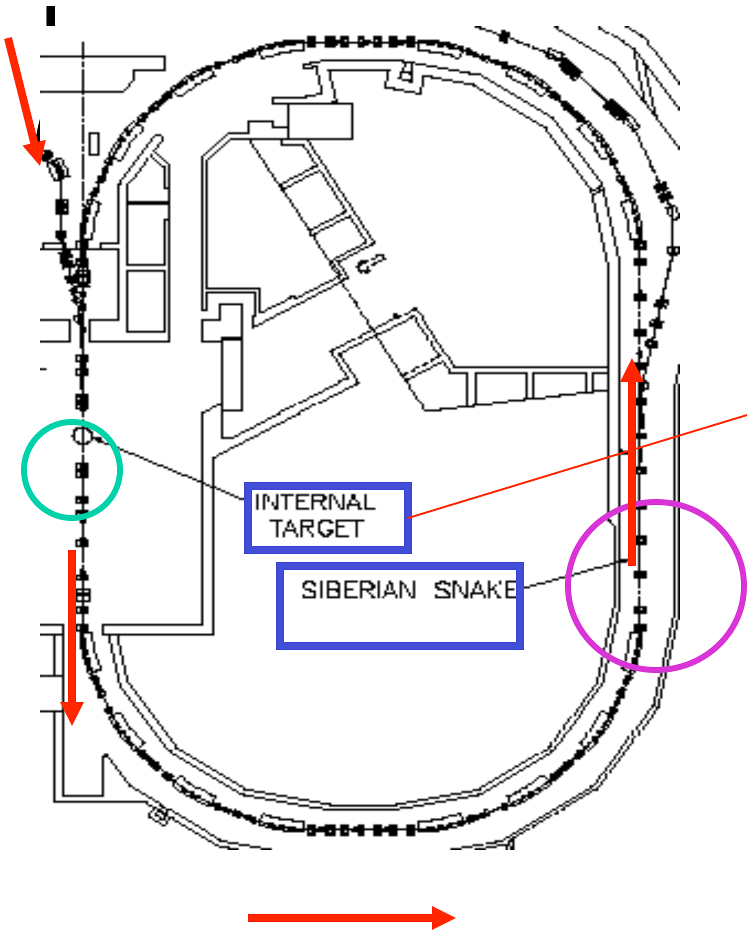


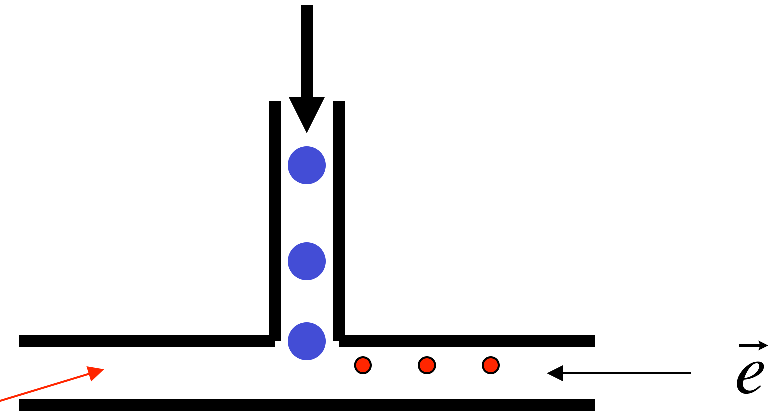


- high polarization
- pure target
- thin cell walls
- low holding field
- **low systematics**

**South Hall Ring**

**L ~ $10^{32}$ electron·atoms $cm^{2}s^{-1}$**

# Stored beam for BLAST

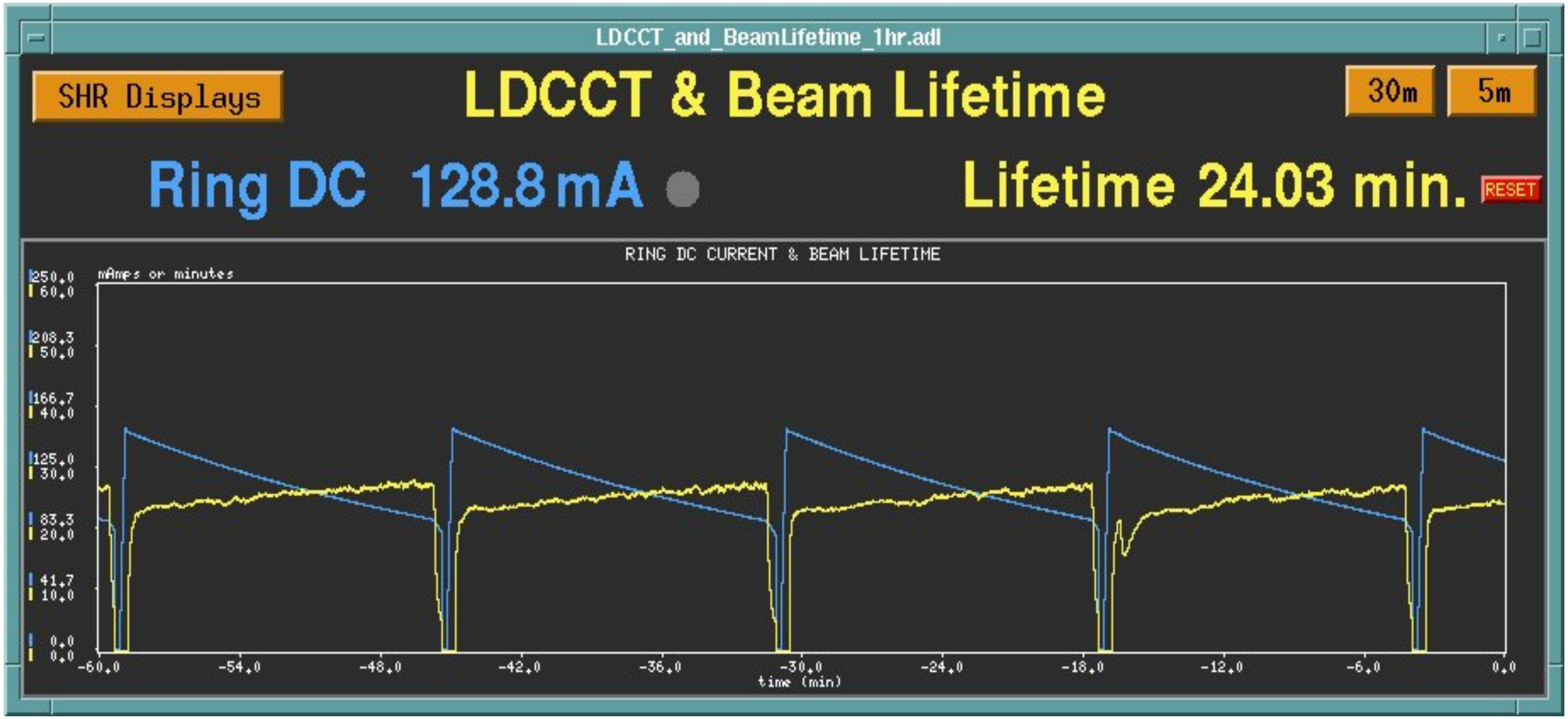


- Accelerator complex and BLAST experiment fully automated
- Stored currents: routinely fill to 225 mA, lifetime of 35 minutes at 100mA
- Beam Polarization: ~65% with possibility of rapid reversal (flipper)

# South Hall Ring Polarization

**Electron beam energy: 850 MeV**

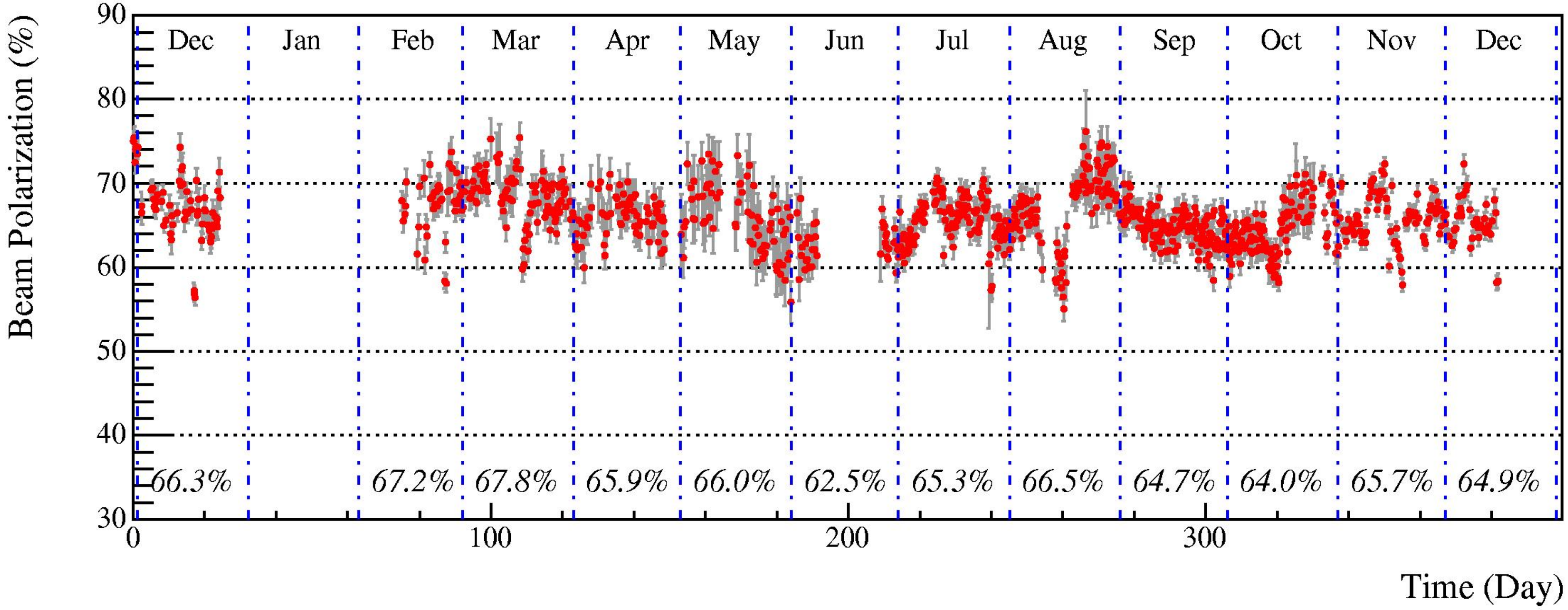


**Compton polarimeter data from Dec. 2003 – Dec. 2004**
**Mean polarization of 66% measured**

# BLAST Detector

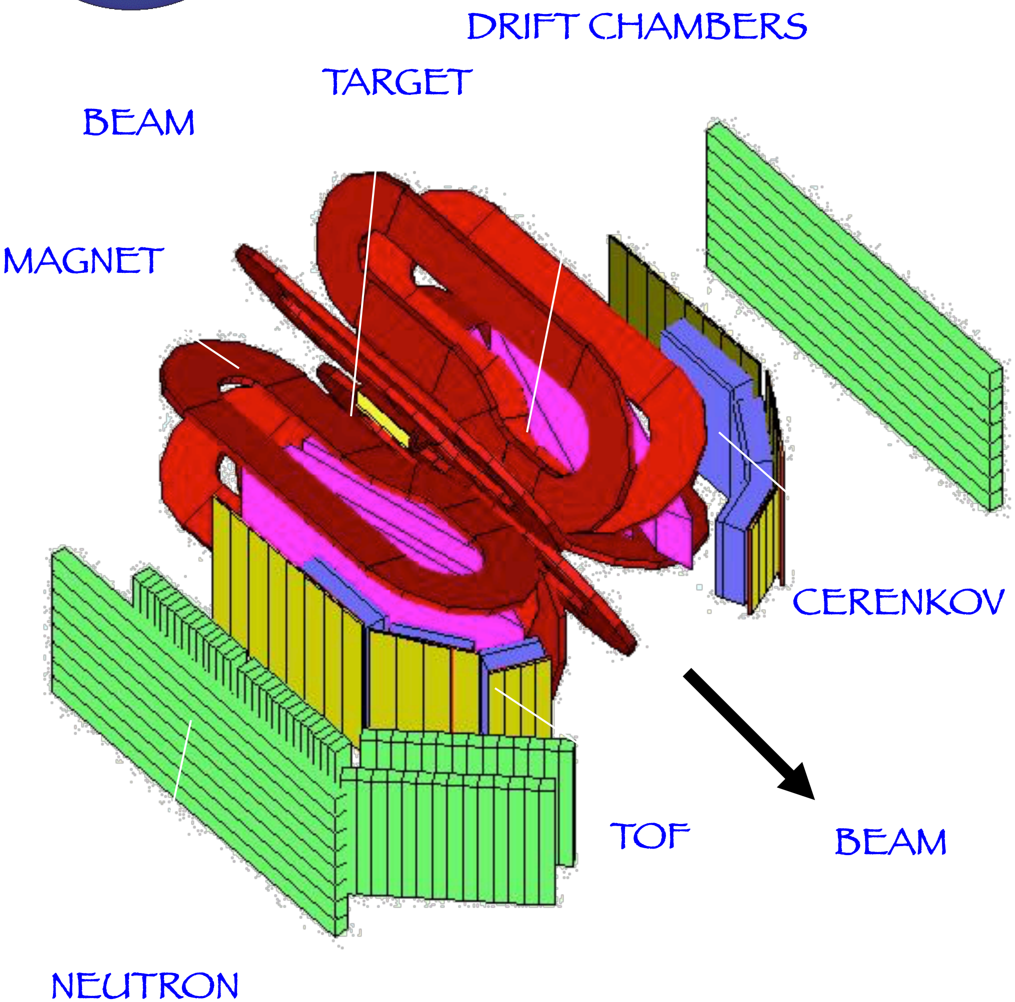


- Toroidal magnetic field
  - 3.8 kG max
- Drift Chambers
  - 3 chambers/sector
  - 2 superlayers/chamber (±5°)
  - 3 sense layers/superlayer
  - 18 tracking layers/sector
  - 954 sense wires
- Cerenkov Detectors
  - 1 cm thick aerogel
  - Electron identification
- Time of flight scintillators
  - 16 vertical bars, 2.5 cm thick
  - Trigger and relative timing
- Neutron detectors
  - 10 cm thick in left sector
  - 25-30 cm thick in right sector
- 2 level, 8 channel trigger system
  - Concurrent data acquisition

# BLAST Toroid

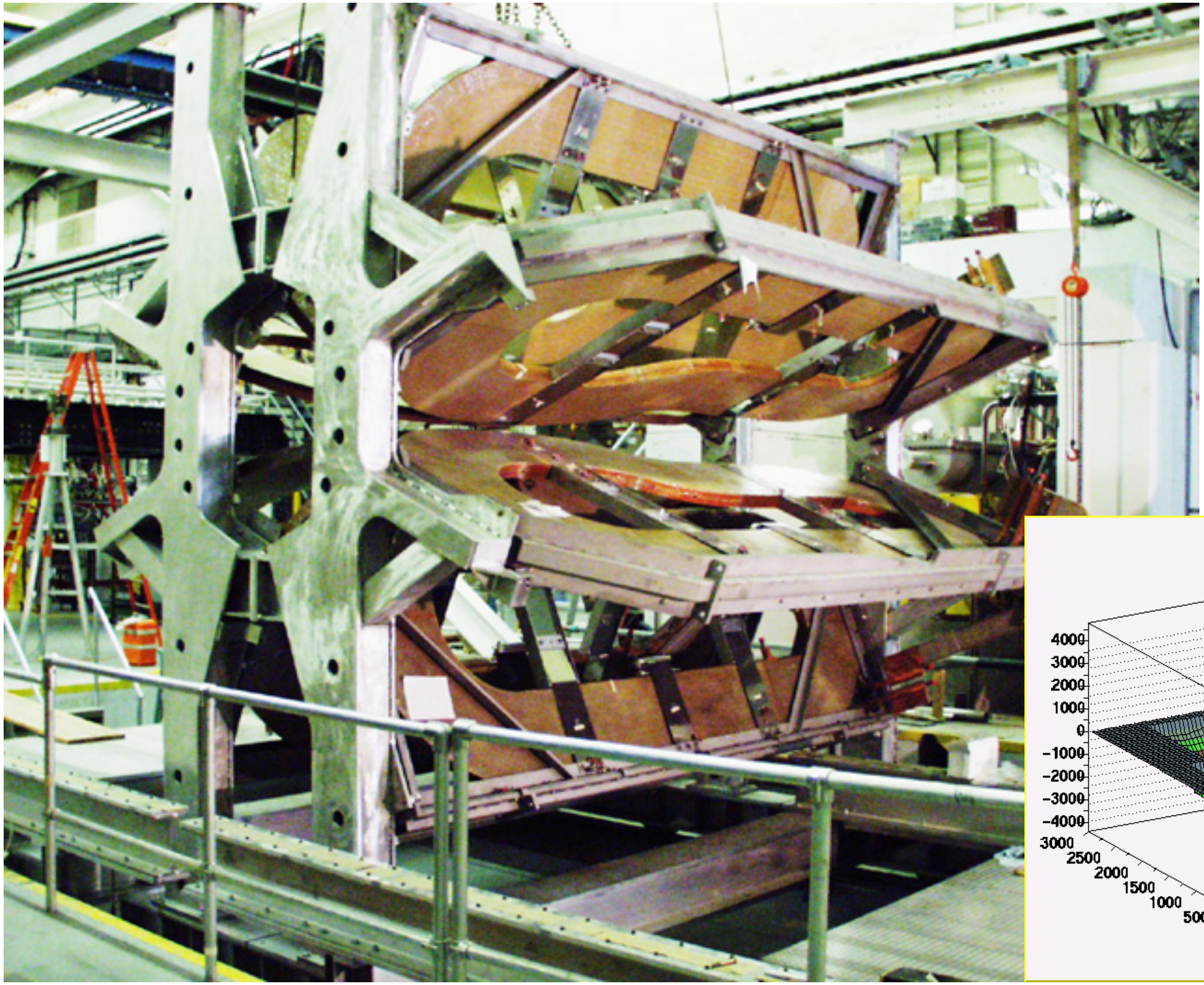

- 8 copper coils
  - 6730 A
  - 3700 G
- field mapped (3D)
  - coil position adjusted
  - ±1% of calculated
  - minimize target field
  - tracking

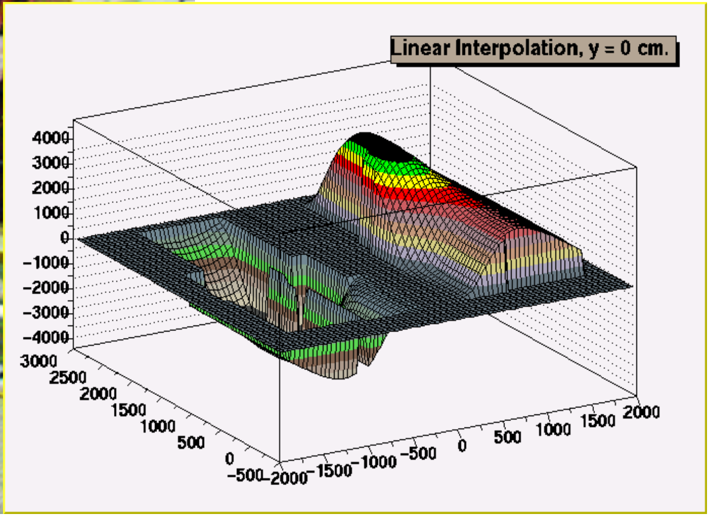

# BLAST Polarized $^{2}$H Target

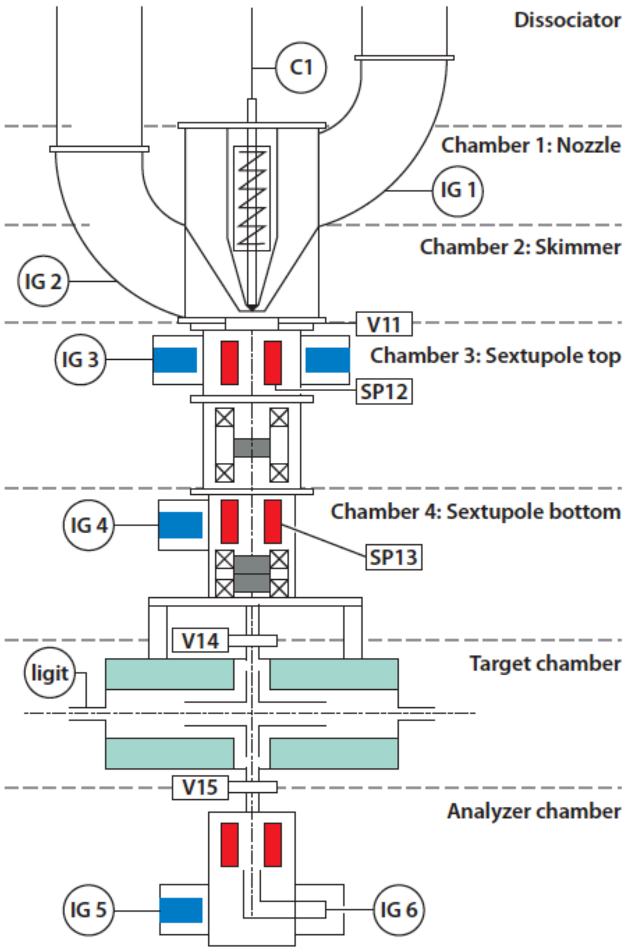


D. Cheever *et al*., Nucl. Instr. Meth. A **556**, 410 (2006)

- Atomic beam source embedded in ≈2 kG BLAST toroidal magnetic field
- Required custom shielding of many components
- Flux: 5 x $10^{16}$ atoms/sec
- Drifilm coated, cryogenically cooled target cell
- Cycled through $M_s$ sub-states
- Target spin-states switched every 5 minutes
- h = 0.656±0.007(stat)±0.04 (sys)
- hPz = 0.580±0.0034 (stat)±0.0054(sys)
- Pzz = 0.683±0.015(stat)±0.013(sys)

# H & D2 collected charge for BLAST, 2004-2005 = 3.25 MegaCoulomb

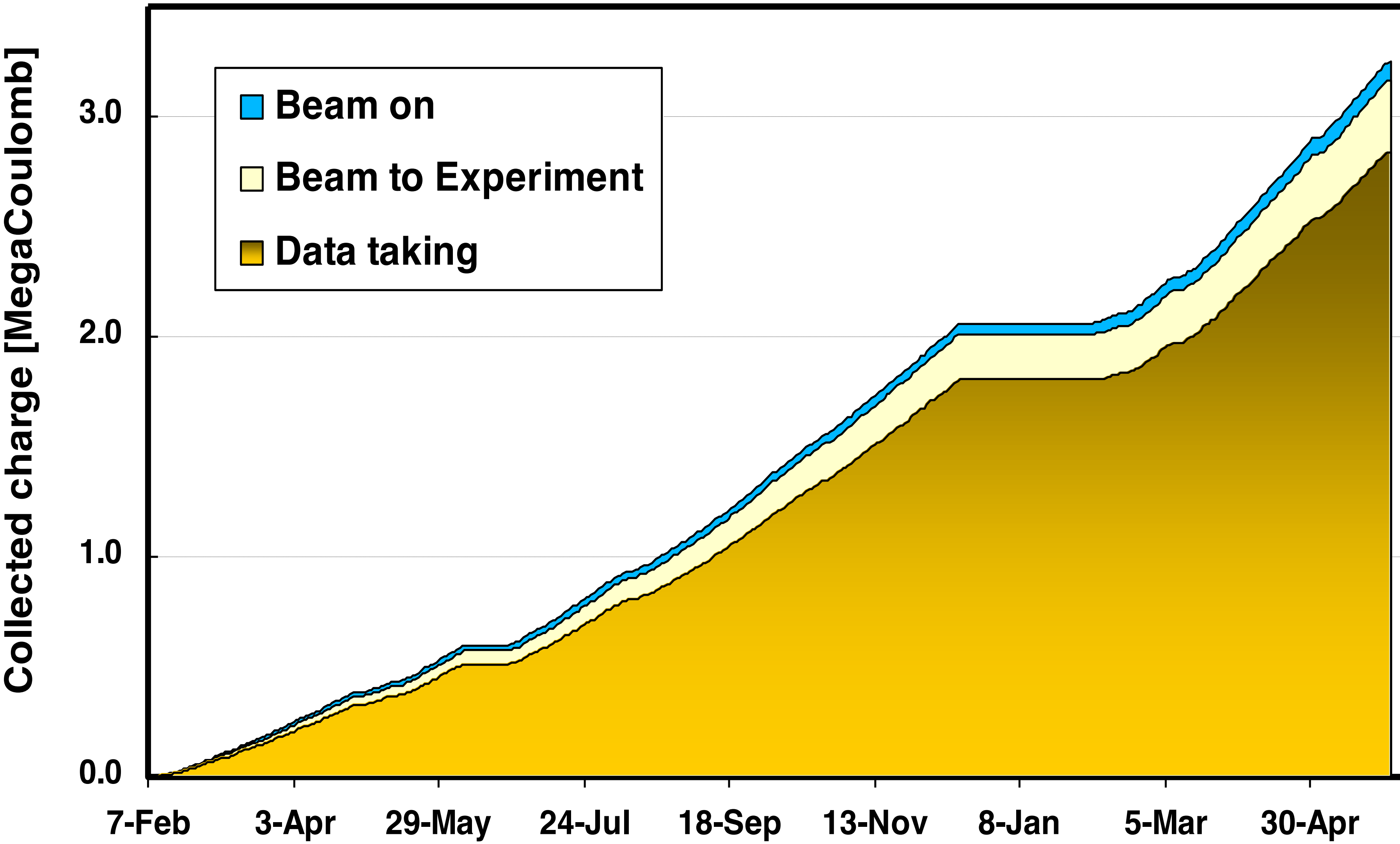

# Elastic Electron Scattering Primer

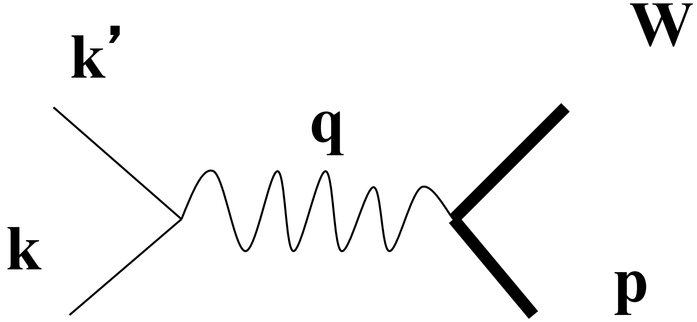


$Q^2 \equiv -q \cdot q > 0$

$\nu \equiv E - E'$

$Q^2 = 4\, EE' \sin^2 \theta/2$

$x = Q^2/2M\nu$

$$W^2 = (q + p)^2 = M^2 + 2M\nu - Q^2$$

Elastic scattering: $W^2 = M^2 \Rightarrow Q^2 = 2\, M\nu$

$$\frac{d\sigma}{d\Omega} = \left(\frac{d\sigma}{d\Omega}\right)_{Mott} \bullet \left[\frac{G_E^{p2} + \tau G_M^{p2}}{1+\tau} + 2\tau G_M^{p2} \tan^2\frac{\theta}{2}\right]$$

# BLAST scientific motivation: nucleon and nuclear structure at low $Q^2$

- Pion is essential to understanding both nucleon and nuclear structure
- In low energy elastic electron-nucleon scattering one would expect effects of mesons to occur at

  $r \sim 2$ fermi => $Q^2 \sim 0.1\ (\text{GeV}/c)^2$
- Search for effects of meson cloud on long distance structure of nucleon
- Seek precise determination of neutron electric form factor with low systematic uncertainties
- Spin structure of deuterium is a stringent test of our understanding of the nucleon-nucleon interaction in nuclei
- **Optimal experimental technique**: precision experiments possible using polarized gas target internal to electron storage ring

# Polarized Elastic Electron Scattering

- In elastic scattering, polarizing both the electron and the target proton, allows determination of the ratio $G_E/G_M$ with low systematic uncertainty.
- With a tensor polarized deuteron target, elastic scattering yields $T_{20}$.
- With a vector polarized deuteron target, and by detecting the neutron in coincidence, the ratio $G_E/G_M$ can be determined for the neutron.
- Spin is used as a "knob" to access scattering from the neutron.
- By detecting quasielastic $^2$H(e,e'n) scattering, $G^n_E(Q^2)$ was determined at MIT-Bates at low $Q^2$ using the Bates Large Acceptance Spectrometer Toroid (BLAST).

# Charge distribution of neutron

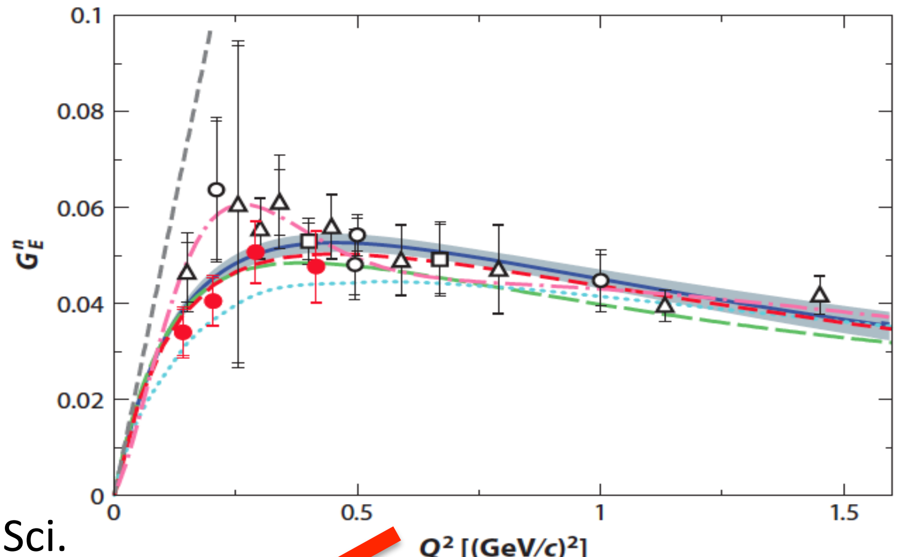


E. Geis *et al.*,
Phys. Rev. Lett. **101**,
042501 (2008)

D.K. Hasell *et al.*,
Ann. Rev. Nucl. and Part. Sci.
**61**, 409 (2011)

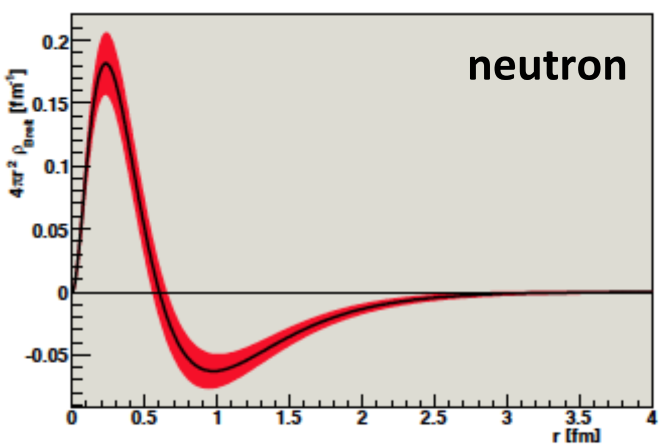


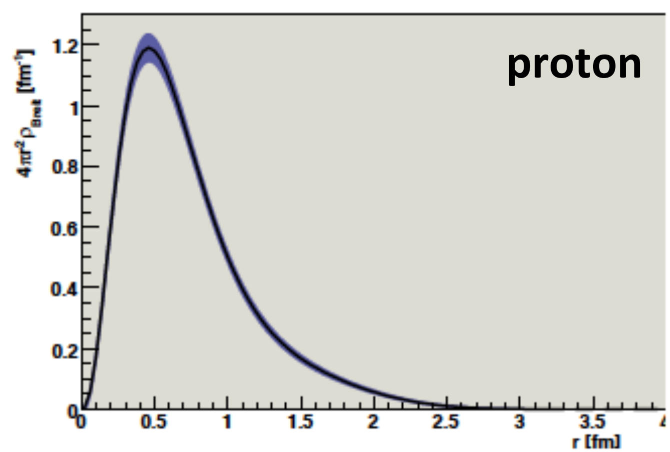


**Highlighted in**

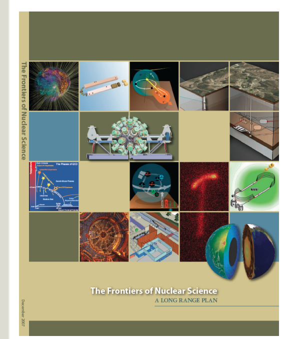

# Interpretation of Neutron Charge Distribution

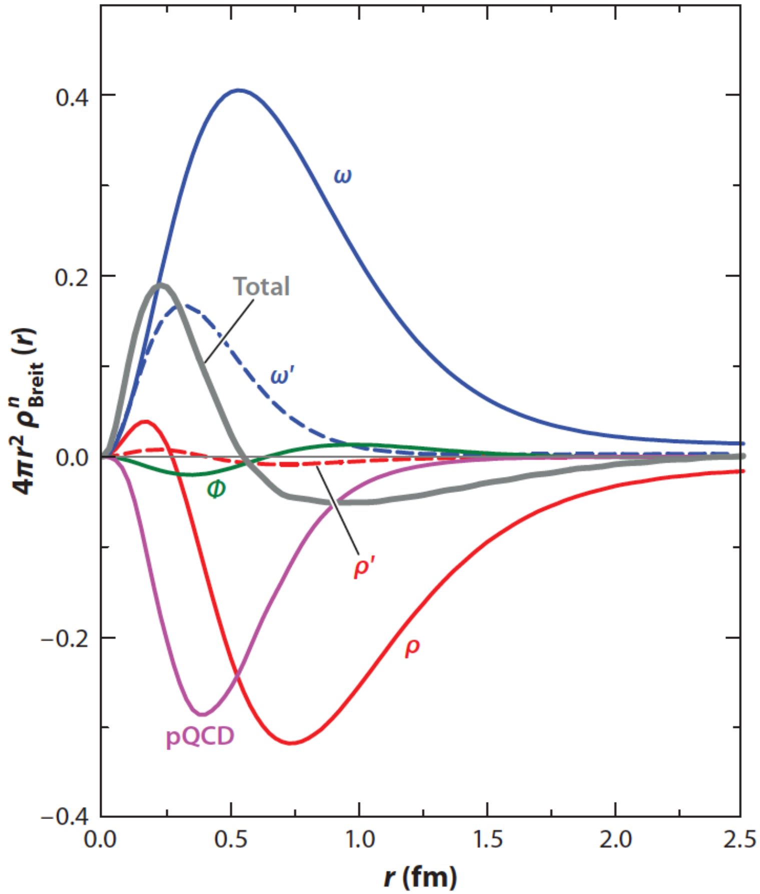


**Figure 9**

$4\pi r^2 \rho^n_{\mathrm{Breit}}(r)$ showing the relative contributions of the various vector mesons from the GKex model together with the perturbative quantum chromodynamics (pQCD) contribution.

# Precision measurement of deuteron tensor analyzing powers with BLAST

C. Zhang *et al.*,
Phys. Rev. Lett. **107**, 252501 (2011)

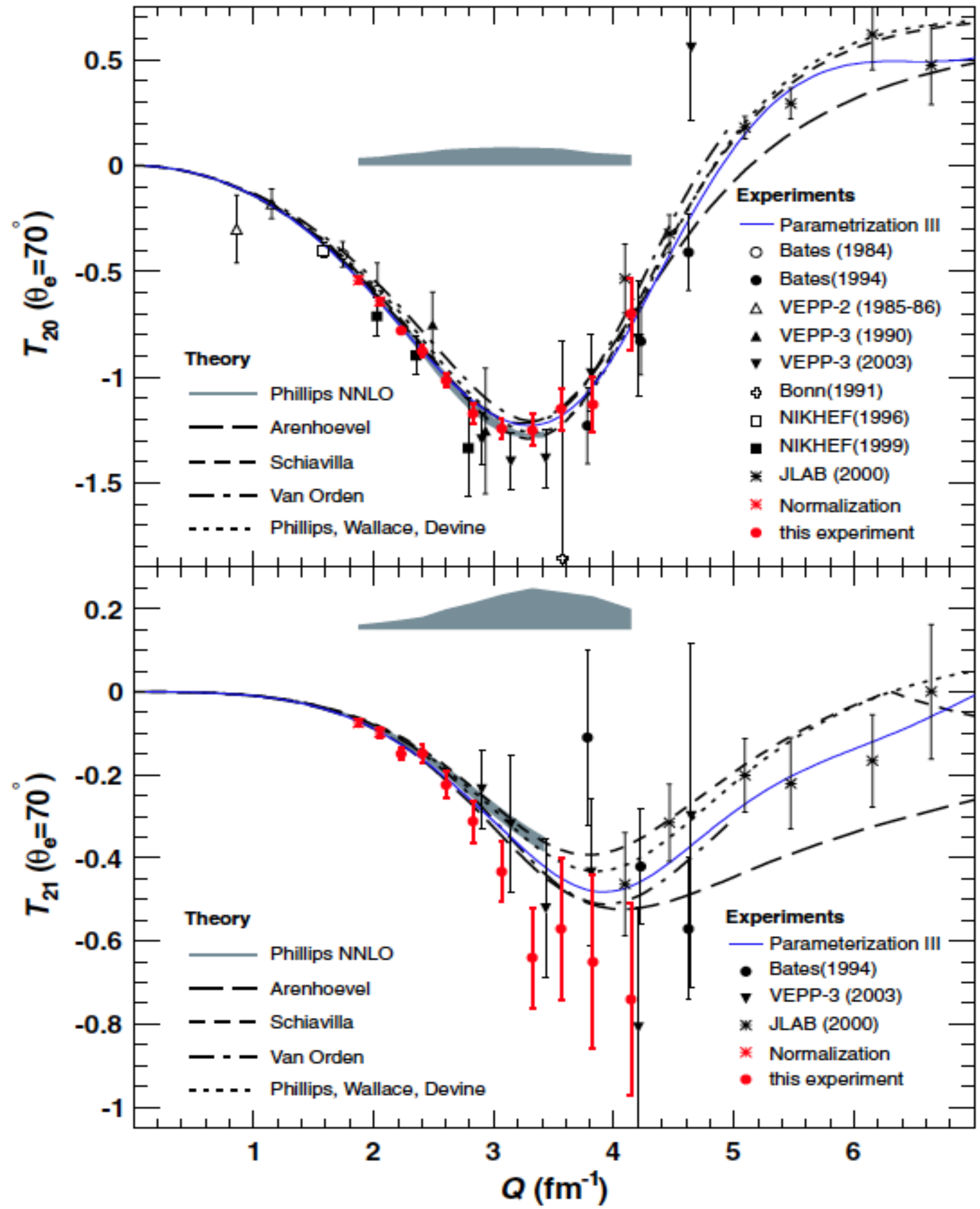


Precision data validate effective field theory

# Quasielastic $^2$H(e,e'p) Reaction

**Cross section**

$$\frac{d\sigma}{d\omega d\Omega_e d\Omega_{pn}^{CM}} = S_0[1 + P_z A_d^V + P_{zz} A_d^T$$
$$+ h(A_e + P_z A_{ed}^V + P_{zz} A_{ed}^T)]$$

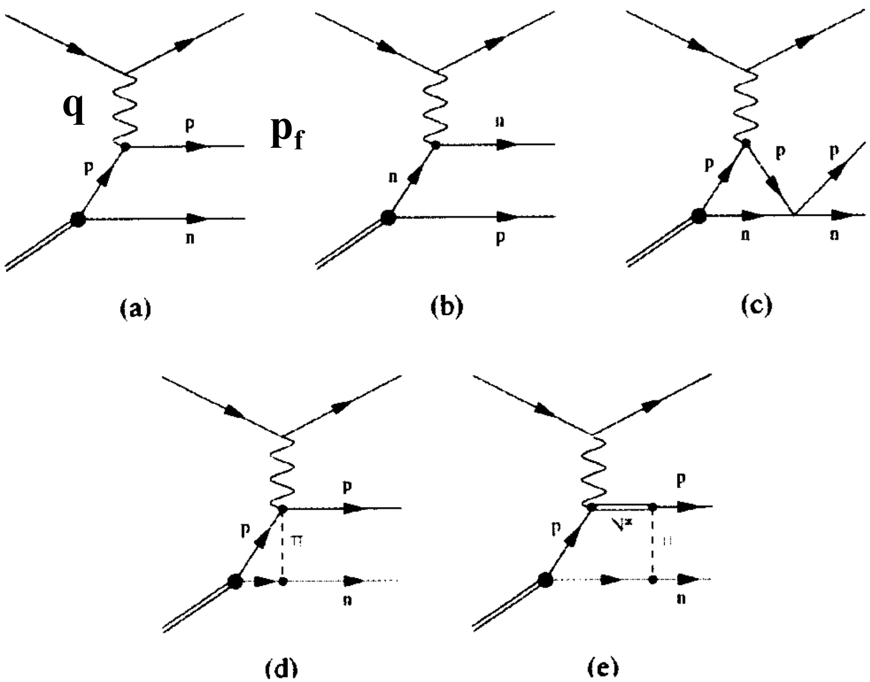


**Missing momentum**

$$\boldsymbol{p}_m \equiv \boldsymbol{q} - \boldsymbol{p}_f$$

- Electron beam polarized
- $^2$H both vector and tensor pol.
- **q** and $\mathbf{p_f}$ and thus $\mathbf{p_m}$ determined by BLAST spectrometer
- Large acceptance => $p_m$ measured up to 500 MeV/c
- Data taking simultaneous with $G^n_E$ and $T_{20}$ measurements

# Quasielastic $^2$H(e,e'p) Data Taking

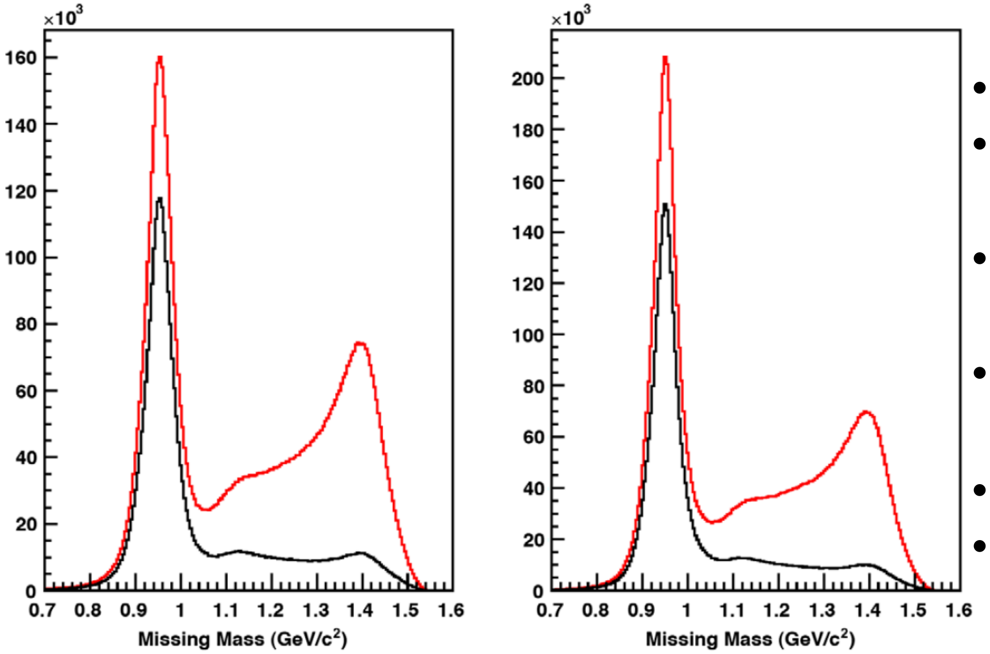


FIG. 1. Histograms of the yields versus missing mass for target spin angle ≈31° without (red) and with (black) Čerenkov cuts for $0.1 < Q^2 < 0.5$ (GeV$/c)^2$ for *opposing* (left) and *same* (right) sector kinematics.

- Data taken in two separate running periods
- Simultaneous with BLAST measurements of $G^n_E$ and $T_{20}$
- Average target spin angles were 31.3±0.43° and 47.4±0.45°
- Target spin angle was in horizontal plane pointing into the left sector
- Determined using $T_{20}$ data
- Electrons scattered into the right (left) sector delivered momentum transfer predominantly parallel (perpendicular) to the target spin vector, the so-called *same sector* (*opposing sector*) kinematics

# Quasielastic $^2$H(e,e'p) Vector Asymmetries

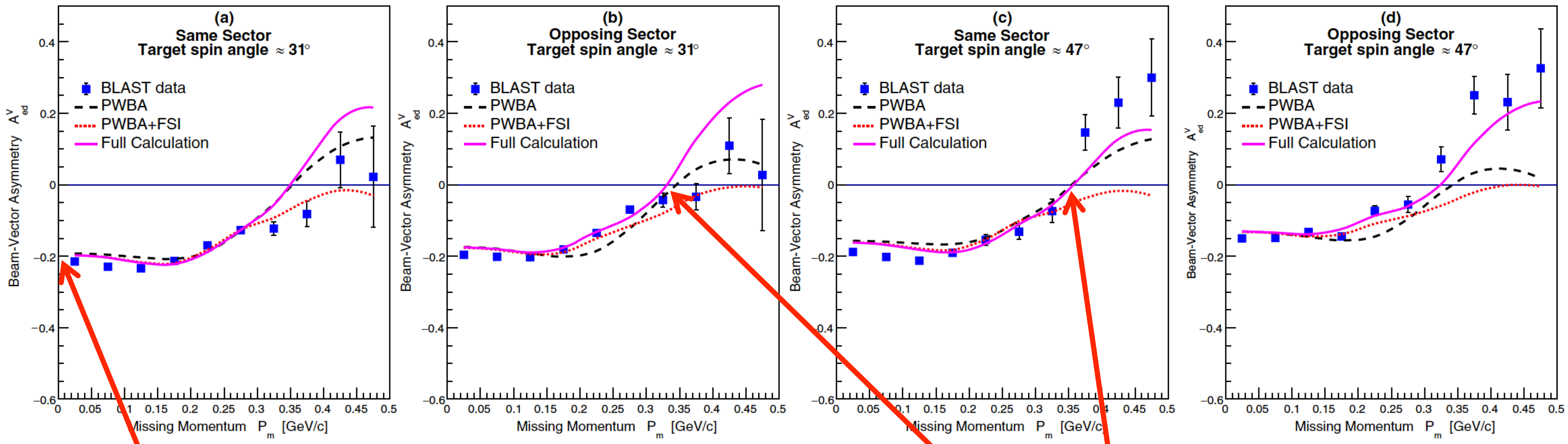


FIG. 2. Beam-vector asymmetries $A^V_{ed}$ for $0.1 < Q^2 < 0.5$ $(\mathrm{GeV}/c)^2$ vs $p_m$. Panels (a) and (c) refer to *same sector* kinematics for target spin angles ≈31° and ≈47°. Panels (b) and (d) refer to *opposing sector* kinematics for the same target spin angles.

**$A^V_{ed} \approx hP_z$ at $p_m = 0$**

$$P = \sqrt{\frac{2}{3}} P_z \left( P_S - \frac{1}{2} P_D \right)$$

**Zero crossing at about 320 MeV/c**

# Quasielastic $^2H(e,e'p)$ Tensor Asymmetries

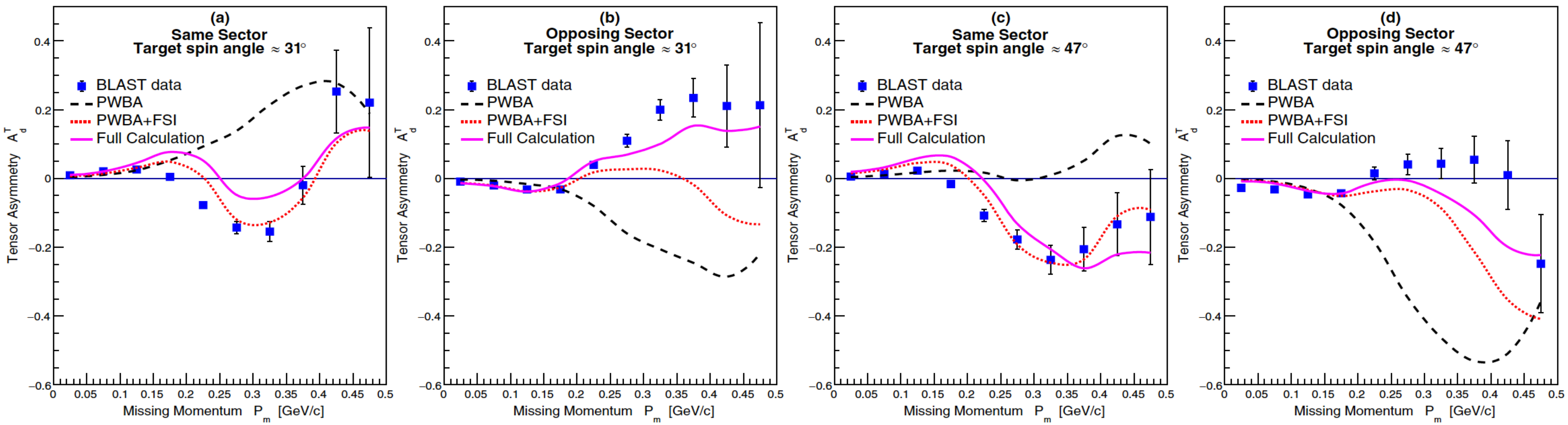


FIG. 3. Tensor asymmetries $A_d^T$ for $0.1 < Q^2 < 0.5$ $(\text{GeV}/c)^2$ vs $p_m$. Panels (a) and (c) refer to *same sector* kinematics for target spin angles ≈32° and ≈47°. Panels (b) and (d) refer to *opposing sector* kinematics for the same target spin angles.

- At low $p_m$, S-state dominates so $A^T_d$ is small
- At high $p_m$, D-state dominates
- However, at high $p_m$ there is a strong influence of FSI: tensor component of NN force

# Summary

- Newly published data are reported for $A^V_{ed}$ and $A^T_d$ spin asymmetries for $0.1 < Q^2 < 0.5$ (GeV/c)$^2$.
- Mapped out in quasielastic kinematics $^2$H(e,e'p) over
  $0 < p_m < 500$ MeV/c.
- Polarized electron beam incident on vector and tensor polarized $^2$H target.
- Large acceptance detector allows large range in $Q^2$ and $p_m$.
- D-state contribution is clearly evident as $p_m$ increases.
- $A^V_{ed}$ has a zero crossing at $p_m \approx 320$ MeV/c, as predicted.
- $A^T_d$ in same and opposing sector kinematics probe the proton-neutron interaction over a large spatial range.
- Theoretical understanding validated by experiment.